PHYSICAL REVIEW A VOLUME 16, NUMBER 3 SEPTEMBER 1977

# Many-body calculation on the photoionization of neon and argon isoelectronic sequences

T. N. Chang
*Physics Department, The University of Southern California, Los Angeles, California 90007*
(Received 29 November 1976)

This paper presents the results of a calculation on the photoionization of Ne and Ar isoelectronic sequences based on a recently developed many-body theory of atomic transitions. Within this theoretical approach, one is able to concentrate attention on studies of the systematics of various many-body effects and of their implications for the photoionization process along isoelectronic sequences. The transition-matrix elements obtained with different degrees of approximation are given in detail. The photoionization cross sections and the asymmetry parameter representing the photoelectron angular distribution are also given. In addition, this study indicates that the usual effective ionization mechanism for the neutral atom, namely, the direct ionization of the outer-shell electron at relatively low energies, becomes ineffective for the ion systems as the degree of ionization increases along the isoelectronic sequence.

## I. INTRODUCTION

In the past few years, it has become evident that the basic information concerning the atomic transitions have played an increasingly important role in the area of energy-related research. For instance, reliable atomic data, such as the transition probabilities and the wavelengths of the strong resonant lines of the isoelectronic sequences of heavy elements, are particularly important in the development of the plasma diagnostic technique.[1]

Unfortunately, most of the investigations, especially on the experimental side, have been concentrated on the neutral atoms. With the possible exception of the beam-foil spectroscopy,[2] only limited efforts have been made on the study of the transitions of atomic-ion systems. This is mainly due to the lack of adequate ion sources which are essential in securing reliable experimental data. Only in the recent few months, several experiments with more reliable quantitative data have been reported.[3,4] In a laser-produced plasma column, Lucatorto and McIlrath[3] have measured the absorption spectrum of $Na^+$ ion. Using a beam-foil time-of-flight method, Pegg *et al.*[4] have measured quantitatively the radiative lifetimes and transition probabilities for electric dipole $\Delta n = 0$ transition in highly stripped sulfur ions.

On the theoretical side, two specific areas are of particular importance: (i) the direct computation of reliable atomic transition data, and (ii) the study of the ionization mechanism of an ion system which in turn can provide an effective procedure in the production of an adequate ion source for the detailed laboratory investigations. In this paper, we report the result of a calculation on the photoionization of the isoelectronic sequences of neon and argon as the first step of a systematic attempt to achieve the main objectives in these two areas.

The theoretical approach employed in this calculation is based on a recent reformulation of the many-body theory of atomic transitions.[5,6] The reliability and the computational efficiency of this approach have been demonstrated in its application on the photoionization of neon and argon[7] where excellent agreement between the theoretical estimation and the experimental measurement is obtained for the photoionization cross section and for the angular distribution of the photoelectron. In this paper, we will concentrate our attention on the studies of the systematics as well as of the influence of many-body effects along the isoelectronic sequence and on their implications for the understanding of the ionization mechanism for the ion systems.

## II. CALCULATIONAL PROCEDURE

The detailed formulation of the theoretical approach used in our calculation is given in Refs. 5 and 6 and a brief summary of the calculational procedure in Ref. 7. The photoionization cross sections for the $np \to kl$ transition in the dipole-velocity and dipole-length approximations are

$$\sigma^V = \frac{16(2l+1)(2\pi\alpha)}{k}(k^2+\epsilon_I)^{-1}\begin{pmatrix} l & 1 & 1 \\ 0 & 0 & 0 \end{pmatrix}^2 \times (5.29\times 10^{-9})^2 |D^V|^2 \text{ cm}^2, \quad (1)$$

$$\sigma^L = \frac{4(2l+1)(2\pi\alpha)}{k}(k^2+\epsilon_I)\begin{pmatrix} l & 1 & 1 \\ 0 & 0 & 0 \end{pmatrix}^2 \times (5.29\times 10^{-9})^2 |D^L|^2 \text{ cm}^2, \quad (2)$$

where $\epsilon_I$ is the ionization energy. In the present calculation, $\epsilon_I$ is given by the single-particle Hartree-Fock orbit energy. The dipole matrix element $D$ is given by

$$D = T_0 + T_1, \quad (3)$$

with

$$T_0 = \langle \chi_{np} | d | \psi_l \rangle \quad \text{and} \quad T_1 = -\langle \phi_l | d | \chi_{np} \rangle , \tag{4}$$

where $d$ is the dipole operator and $\chi_{np}$ is the ground state Hartree-Fock radial wave function for the outermost shell $np$. The single-particle radical functions $\psi_l$ and $\phi_l$ satisfy the set of coupled equations (2a) and (2b) of Ref. 7. The angular distribution of the photoelectron, represented by the asymmetry parameter $\beta_{np}$, is calculated by the procedure of Cooper and Zare.[8,9]

Following Ref. 7, the present calculation has also been carried out in three steps which correspond to the single-particle approach (I), the many-body perturbation theory[10] (II), and the random-phase approximation (III). Four elements in each isoelectronic sequence (Ne, $Na^+$, $Mg^{++}$, and $Al^{+++}$ in Ne sequence, and Ar, $K^+$, $Ca^{++}$, and $Sc^{+++}$ in Ar sequence) are included.

## III. Ar ISOELECTRONIC SEQUENCE

Table I presents the calculated values of the dipole matrix elements $D$ for the $3p \rightarrow kd$ transition at three selected photoelectron momenta $k = 0.2$, 1.4, and 2.6 in the dipole-velocity ($V$) and dipole-length ($L$) approximations. In order to study the detailed variation of the dipole matrix elements in different approximations, we have listed in Table I the results of three different approaches which correspond to the three steps (I, II, and III) of our calculation. For the $3p \rightarrow ks$ transition, the detailed values for the dipole matrix elements are not listed since the results of II and III deviate very little from that of I and the results of the velocity and length calculations also agree well with each other. Table II presents the partial cross sections $\sigma_s$ and $\sigma_d$ for transitions $3p \rightarrow ks$ and $3p \rightarrow kd$ in the dipole velocity approximation. Similar results using the dipole-length approximations are given in Table III.

Figures 1 and 2 give the partial photoionization cross sections from the $3p$ shell for photoelectron energies up to 120 eV. Only the results of two steps, step I (dashed line) and step III (solid line), are included. We should also point out that at lower energies, the velocity and length results of step III for Ar and $K^+$ are indistinguishable on the scale given in Fig. 1. Figure 3 gives the results of the photoelectron angular distribution of the $3p$ electron represented by the asymmetry parameter $\beta_{3p}$. For $K^+$, $Ca^{++}$, and $Sc^{+++}$, the variation of the photoelectron angular distribution for I, II, and III follows closely to that of Ar discussed

TABLE I. Dipole matrix elements $D$ [Eq. (4)] for the $3p \rightarrow kd$ transition for Ar, $K^+$, $Ca^{++}$, and $Sc^{+++}$ at the photoelectron momenta $k = 0.2$, 1.4, and 2.6. $V$ ($L$) stands for the dipole-velocity (-length) approximation. The calculations were carried out in steps in the single-particle approach (I), many-body perturbation theory (II), and the random-phase approximation (III).

| | | | Ar | | $K^+$ | | $Ca^{++}$ | | $Sc^{+++}$ | |
|---|---|---|---|---|---|---|---|---|---|---|
| $k$ | Step | | $T_0$ | $T_1$ | $T_0$ | $T_1$ | $T_0$ | $T_1$ | $T_0$ | $T_1$ |
| 0.2 | I | $V$ | −0.529 | 0.0 | −0.904 | 0.0 | −0.283 | 0.0 | 0.130 | 0.0 |
| | | $L$ | 1.135 | 0.0 | 1.078 | 0.0 | 0.267 | 0.0 | −0.016 | 0.0 |
| | II | $V$ | −0.529 | −0.068 | −0.904 | −0.134 | −0.283 | −0.078 | 0.130 | −0.030 |
| | | $L$ | 1.135 | −0.100 | 1.078 | −0.149 | 0.267 | −0.072 | −0.016 | −0.024 |
| | III | $V$ | −0.606 | −0.084 | −0.898 | −0.145 | −0.198 | −0.068 | 0.147 | −0.027 |
| | | $L$ | 1.252 | −0.122 | 1.036 | −0.162 | 0.189 | −0.063 | −0.031 | −0.022 |
| 1.4 | I | $V$ | −0.590 | 0.0 | 0.118 | 0.0 | 0.558 | 0.0 | 0.831 | 0.0 |
| | | $L$ | 0.750 | 0.0 | 0.079 | 0.0 | −0.150 | 0.0 | −0.215 | 0.0 |
| | II | $V$ | −0.590 | −0.175 | 0.118 | −0.090 | 0.558 | −0.041 | 0.831 | −0.016 |
| | | $L$ | 0.750 | −0.243 | 0.079 | −0.101 | −0.150 | −0.041 | −0.215 | −0.016 |
| | III | $V$ | −0.435 | −0.154 | 0.173 | −0.081 | 0.575 | −0.039 | 0.835 | −0.015 |
| | | $L$ | 0.545 | −0.215 | 0.017 | −0.092 | −0.168 | −0.038 | −0.220 | −0.015 |
| 2.6 | I | $V$ | 1.041 | 0.0 | 1.173 | 0.0 | 1.293 | 0.0 | 1.397 | 0.0 |
| | | $L$ | −0.299 | 0.0 | −0.289 | 0.0 | −0.273 | 0.0 | −0.254 | 0.0 |
| | II | $V$ | 1.041 | 0.017 | 1.173 | 0.018 | 1.293 | 0.019 | 1.397 | 0.021 |
| | | $L$ | −0.299 | 0.018 | −0.289 | 0.015 | −0.273 | 0.013 | −0.254 | 0.011 |
| | III | $V$ | 1.041 | 0.017 | 1.173 | 0.018 | 1.292 | 0.019 | 1.397 | 0.020 |
| | | $L$ | −0.297 | 0.018 | −0.288 | 0.015 | −0.272 | 0.013 | −0.253 | 0.011 |

TABLE II. Partial photoionization cross sections (in units of Mb) for the $3p \rightarrow ks$ ($\sigma_s$) and $3p \rightarrow kd$ ($\sigma_d$) transitions in the dipole-velocity calculation.

| | | Ar | | $K^+$ | | $Ca^{++}$ | | $Sc^{+++}$ | |
|---|---|---|---|---|---|---|---|---|---|
| $k$ | Step | $\sigma_s$ | $\sigma_d$ | $\sigma_s$ | $\sigma_d$ | $\sigma_s$ | $\sigma_d$ | $\sigma_s$ | $\sigma_d$ |
| 0.2 | I | 3.71 | 15.68 | 1.55 | 23.49 | 0.850 | 1.44 | 0.538 | 0.211 |
| | II | 3.84 | 19.98 | 1.59 | 30.94 | 0.868 | 2.34 | 0.547 | 0.126 |
| | III | 3.85 | 26.65 | 1.59 | 31.24 | 0.868 | 1.28 | 0.547 | 0.181 |
| 0.5 | I | 2.75 | 19.63 | 1.31 | 18.33 | 0.764 | 0.534 | 0.499 | 0.323 |
| | II | 2.85 | 25.35 | 1.34 | 24.67 | 0.779 | 1.00 | 0.507 | 0.230 |
| | III | 2.85 | 34.01 | 1.34 | 20.56 | 0.779 | 0.498 | 0.507 | 0.286 |
| 0.8 | I | 1.74 | 21.84 | 0.993 | 7.60 | 0.635 | 0.014 | 0.436 | 0.518 |
| | II | 1.80 | 28.90 | 1.02 | 10.82 | 0.647 | 0.094 | 0.443 | 0.430 |
| | III | 1.80 | 34.97 | 1.02 | 7.07 | 0.647 | 0.020 | 0.443 | 0.475 |
| 1.1 | I | 1.04 | 13.11 | 0.707 | 0.885 | 0.499 | 0.157 | 0.363 | 0.740 |
| | II | 1.07 | 18.23 | 0.724 | 1.54 | 0.508 | 0.082 | 0.369 | 0.674 |
| | III | 1.07 | 14.42 | 0.724 | 0.849 | 0.508 | 0.129 | 0.369 | 0.701 |
| 1.7 | I | 0.387 | 0.093 | 0.336 | 0.476 | 0.280 | 0.819 | 0.229 | 1.005 |
| | II | 0.395 | 0.042 | 0.342 | 0.411 | 0.284 | 0.785 | 0.232 | 0.999 |
| | III | 0.395 | 0.071 | 0.342 | 0.440 | 0.284 | 0.798 | 0.232 | 1.002 |
| 2.3 | I | 0.159 | 0.745 | 0.159 | 0.856 | 0.150 | 0.924 | 0.135 | 0.945 |
| | II | 0.162 | 0.757 | 0.162 | 0.872 | 0.152 | 0.943 | 0.137 | 0.967 |
| | III | 0.161 | 0.757 | 0.162 | 0.872 | 0.152 | 0.943 | 0.137 | 0.967 |
| 2.9 | I | 0.071 | 0.612 | 0.078 | 0.683 | 0.080 | 0.720 | 0.079 | 0.730 |
| | II | 0.071 | 0.634 | 0.079 | 0.707 | 0.081 | 0.744 | 0.079 | 0.754 |
| | III | 0.071 | 0.633 | 0.079 | 0.706 | 0.081 | 0.744 | 0.079 | 0.754 |

TABLE III. Partial photoionization cross sections (in units of Mb) for the $3p \rightarrow ks$ ($\sigma_s$) and $3p \rightarrow kd$ ($\sigma_d$) transitions in the dipole-length calculation.

| | | Ar | | $K^+$ | | $Ca^{++}$ | | $Sc^{+++}$ | |
|---|---|---|---|---|---|---|---|---|---|
| $k$ | Step | $\sigma_s$ | $\sigma_d$ | $\sigma_s$ | $\sigma_d$ | $\sigma_s$ | $\sigma_d$ | $\sigma_s$ | $\sigma_d$ |
| 0.2 | I | 3.92 | 26.96 | 1.80 | 47.38 | 0.936 | 4.63 | 0.580 | 0.024 |
| | II | 3.80 | 22.42 | 1.76 | 35.17 | 0.915 | 2.48 | 0.569 | 0.150 |
| | III | 3.80 | 26.70 | 1.76 | 31.19 | 0.915 | 1.03 | 0.569 | 0.261 |
| 0.5 | I | 3.04 | 35.06 | 1.51 | 39.39 | 0.834 | 2.30 | 0.535 | 0.096 |
| | II | 2.94 | 28.01 | 1.47 | 27.93 | 0.815 | 1.04 | 0.525 | 0.266 |
| | III | 2.94 | 33.41 | 1.47 | 20.14 | 0.815 | 0.351 | 0.525 | 0.379 |
| 0.8 | I | 2.05 | 44.37 | 1.12 | 18.94 | 0.684 | 0.455 | 0.465 | 0.283 |
| | II | 1.98 | 33.01 | 1.09 | 12.03 | 0.668 | 0.086 | 0.456 | 0.483 |
| | III | 1.97 | 35.01 | 1.09 | 6.53 | 0.668 | 0.001 | 0.455 | 0.582 |
| 1.1 | I | 1.23 | 32.37 | 0.775 | 3.49 | 0.529 | 0.004 | 0.385 | 0.559 |
| | II | 1.18 | 21.14 | 0.751 | 1.63 | 0.516 | 0.102 | 0.377 | 0.743 |
| | III | 1.18 | 14.10 | 0.750 | 0.636 | 0.516 | 0.202 | 0.377 | 0.814 |
| 1.7 | I | 0.405 | 0.001 | 0.347 | 0.283 | 0.291 | 0.728 | 0.241 | 1.026 |
| | II | 0.388 | 0.062 | 0.336 | 0.465 | 0.283 | 0.856 | 0.236 | 1.081 |
| | III | 0.387 | 0.139 | 0.335 | 0.544 | 0.283 | 0.898 | 0.236 | 1.099 |
| 2.3 | I | 0.162 | 0.867 | 0.164 | 0.986 | 0.156 | 1.071 | 0.143 | 1.106 |
| | II | 0.156 | 0.835 | 0.159 | 0.949 | 0.152 | 1.021 | 0.140 | 1.046 |
| | III | 0.156 | 0.839 | 0.159 | 0.951 | 0.152 | 1.020 | 0.140 | 1.043 |
| 2.9 | I | 0.074 | 0.838 | 0.082 | 0.899 | 0.085 | 0.925 | 0.083 | 0.920 |
| | II | 0.072 | 0.709 | 0.080 | 0.778 | 0.083 | 0.815 | 0.082 | 0.820 |
| | III | 0.072 | 0.699 | 0.080 | 0.769 | 0.083 | 0.806 | 0.082 | 0.813 |

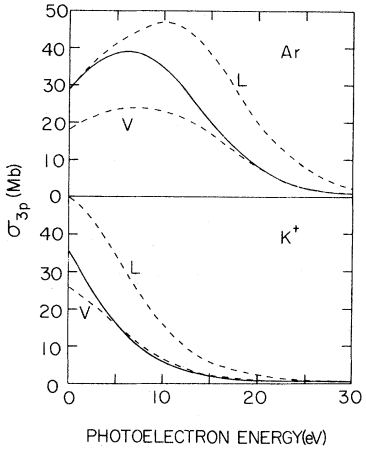


FIG. 1. Partial-photoionization cross section of the $3p$ subshell for Ar and $K^+$. The solid lines represent the results of step III in our calculation. The velocity and length results are practically indistinguishable. The dashed lines represent the results of step I in our calculation.

in Ref. 7. The length and velocity results also agree well with each other and only the results in the step III of the velocity calculations are given. On the high-energy side, we find that the values of $\beta_{3p}$ converge to a constant of about 1.5 for all members in the sequence.

A careful inspection of the calculated data given in Tables I–III and Figs. 1–3 yields several important observations. First, as the energy increases, the difference between the velocity and length calculations based on the single particle calculation (step I) remains significant (~20% at 120 eV). At energies below the Cooper minimum of the

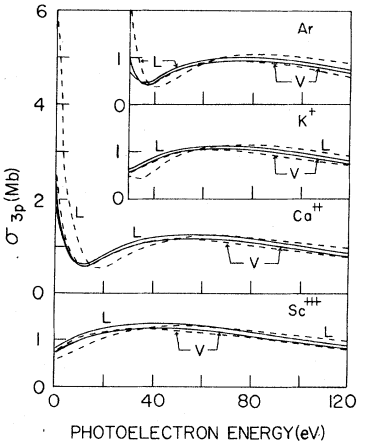


FIG. 2. Partial-photoionization cross section of the $3p$ subshell. The solid lines and the dashed lines represent the results of setp III and step I, respectively. The energy scales for Ar and $K^+$ are the same as that of $Ca^{++}$ and $Sc^{+++}$.

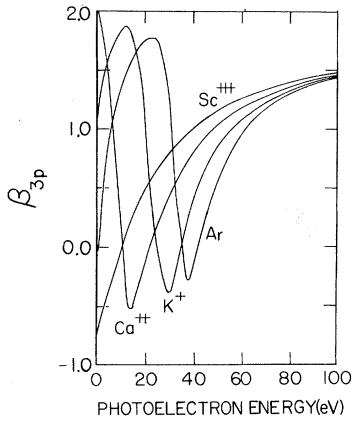


FIG. 3. Asymmetry parameter $\beta_{3p}$ for Ar isoelectronic sequence. Only the velocity results in step III of the present calculation are given.

$3p \rightarrow kd$ transitions, the large differences (as high as 70%) between the velocity and length results in the step I of our calculation are greatly reduced in the step II (to a maximum of about 12%) and almost completely removed in the step III. In contrast, at energies above the Cooper minimum, this difference is reduced by a smaller amount and remains at about 10%. This discrepancy could be attributed to the neglect of coupling with the $3s \rightarrow kp$ transition. The importance of this interchannel interaction between the $3p \rightarrow kd$ and $3s \rightarrow kp$ transitions is anticipated from the fact that the corresponding photoionization cross sections of these two transitions are comparable in this energy region.

Second, since the results of II and III are almost identical at higher energies, it is evident that the effect of the coupling term

$$(l\|V^k(\phi_l, \chi_{np}; r)\|1)\chi_{np}(r) \qquad (5)$$

in Eq. (2a) of Ref. 7 becomes negligible as the energy increases. On the other hand, the difference between II and III is significant on lower energy side and could be even greater for the excitations than for the ionizations. In addition, the difference between the results of I and of III (or II) remains significant even on the higher-energy side. This suggests that the influence of ground state correlations, included in our calculation through the mixing of the $3p^6$ and $3p^4dd'$ configurations, persists even at higher energies.

Third, from Figs. 1 and 2, we find that the broad maximum exhibited in the Ar ionization spectrum is shifted towards the excitation region as the degree of ionization increases along the isoelectronic sequence. This shift of the oscillator strength suggests that the usual effective ionization mechanism for the neutral atoms, namely, the direct

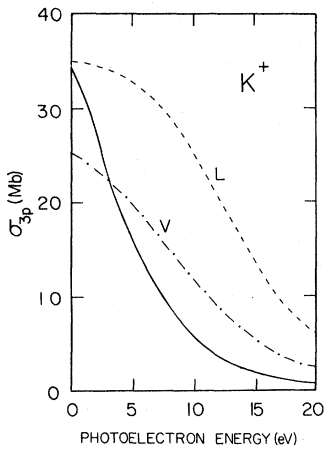


FIG. 4. Comparison between the present calculation and the calculation of Combet Farnoux and Lamoureux (Ref. 13). The solid line represents the results of step III in our calculation where the length and velocity results are indistinguishable. The dashed and the dashed-dotted lines represent the length and velocity results given in Ref. 13 respectively.

ionization of the outer-shell electron at relatively low energy, becomes ineffective for the ion systems. Other ionization mechanisms, such as ionization of an inner-shell electron followed by the Auger transition, may become more favorable. Similar effects in electron-impact ionization processes have also been demonstrated based on simpler single-particle calculations.[11,12]

Next, we compare our results with those of other theoretical calculations. In particular, in a recent calculation, Combet Farnoux and Lamoureux[13] have incorporated the close coupling procedure into the $R$-matrix theory and calculated the partial-photoionization cross section of $K^+$ up to about 100 eV. Figure 4 compares the results of our step III and of Ref. 13. The present calculation yields practically identical velocity and length results, in contrast to a large discrepancy in the data of Ref. 13. Interpretation of this large difference would require access to detailed data analogous to those given in our Tables I–III. More recently, Msezane *et al.*[14] have calculated the photoionization cross sections for all isoelectronic sequences associated with the rare-gas atoms using a multiconfiguration Hartree-Fock approach.[15] Their approach is basically equivalent to the step II of our calculation[7,15] and the results are in excellent agreement.[14]

Systematic experimental data are not available. However, a detailed experimental study seems to be feasible by using the process introduced by Lucatorto and McIlrath,[3] particularly in view of the large cross section near the threshold of $K^+$. The experiment would be even more rewarding if the continuum light source of synchrotron radiation could be used.

## IV. Ne ISOELECTRONIC SEQUENCE

The calculated values of the dipole matrix elements for the $2p \rightarrow kd$ transition and the partial photoionization cross sections $\sigma_s$ and $\sigma_d$ for $2p \rightarrow ks$ and $2p \rightarrow kd$ transitions are given in Tables IV–VI. Figures 5 and 6 give the partial photoionization cross section from the $2p$ shell for photoelectron energies up to 120 eV. Figure 7 presents the asymmetry parameter $\beta_{2p}$ for the photoelectron angular distribution obtained in the step III of the length calculation.

In contrast to the Ar sequence, the Ne sequence yields no Cooper minimum in the $2p \rightarrow kd$ transition. Our calculation shows that the agreement between the velocity and length results is excellent. Also, the $2s \rightarrow kp$ transition is much weaker than the $2p \rightarrow kd$ transition. Thus, the effect of the interchannel interaction between these two transitions on the $2p \rightarrow kd$ transition becomes negligible. We also find that at the lower energies the difference between the results of steps II and III is much smaller than that in the Ar sequence. On the higher-energy side, the effect of this term is negligible as for the Ar sequence. On the other hand, the difference between I and III (or II) remains large at all energies in our calculation. This, of course, demonstrates the importance of including the ground state correlation effect in any theoretical calculation. The shift of oscillator strength to the excitation is also evident but not as distinct as for the Ar sequence. The asymmetry parameters $\beta_{2p}$ also converge to a constant value of about 1.5 at higher energies.

The results of the present calculation for the Ne sequence, in general, agree well with those of other theoretical calculations; for instance, the results of step II in our calculation agree very well with those of Msezane *et al.*[14] Our calculated photoionization cross section for $Na^+$ at the threshold also agrees well with the experimental value ($5.5 \pm 2.5$ Mb) of Lucatorto and McIlrath.[3]

## V. CONCLUSION

The present investigation has clearly demonstrated the need of further exploration of two important areas: (i) the search of other more effective ionization mechanism for the ion systems other than the usual direct ionization of the outershell electron and (ii) the study of the systematics of the oscillator-strength redistribution along the isoelectronic sequence. The extension of the present theoretical approach to the photoexcitation process is straightforward and currently in progress. In

TABLE IV. Dipole matrix elements $D$ [Eq. (4)] for the $2p \rightarrow kd$ transition for Ne, $Na^+$, $Mg^{++}$, and $Al^{+++}$ at photoelectron momenta $k = 0.5$, 1.5, and 2.5.

| | | | Ne | | $Na^+$ | | $Mg^{++}$ | | $Al^{+++}$ | |
|---|---|---|---|---|---|---|---|---|---|---|
| $k$ | Step | | $T_0$ | $T_1$ | $T_0$ | $T_1$ | $T_0$ | $T_1$ | $T_0$ | $T_1$ |
| 0.5 | I | $V$ | −0.580 | 0.0 | −0.866 | 0.0 | −1.049 | 0.0 | −1.150 | 0.0 |
| | | $L$ | 0.693 | 0.0 | 0.517 | 0.0 | 0.381 | 0.0 | 0.282 | 0.0 |
| | II | $V$ | −0.580 | −0.048 | −0.866 | −0.064 | −1.049 | −0.070 | −1.150 | −0.069 |
| | | $L$ | 0.693 | −0.025 | 0.517 | −0.020 | 0.381 | −0.016 | 0.282 | −0.011 |
| | III | $V$ | −0.595 | −0.050 | −0.885 | −0.066 | −1.066 | −0.071 | −1.163 | −0.070 |
| | | $L$ | 0.701 | −0.025 | 0.523 | −0.021 | 0.384 | −0.016 | 0.283 | −0.012 |
| 1.5 | I | $V$ | −1.599 | 0.0 | −1.767 | 0.0 | −1.890 | 0.0 | −1.968 | 0.0 |
| | | $L$ | 0.974 | 0.0 | 0.709 | 0.0 | 0.527 | 0.0 | 0.399 | 0.0 |
| | II | $V$ | −1.599 | −0.146 | −1.767 | −0.138 | −1.890 | −0.129 | −1.968 | −0.120 |
| | | $L$ | 0.974 | −0.065 | 0.709 | −0.041 | 0.527 | −0.027 | 0.399 | −0.019 |
| | III | $V$ | −1.631 | −0.150 | −1.793 | −0.140 | −1.909 | −0.131 | −1.981 | −0.121 |
| | | $L$ | 0.979 | −0.066 | 0.711 | −0.041 | 0.527 | −0.028 | 0.399 | −0.019 |
| 2.5 | I | $V$ | −1.956 | 0.0 | −2.108 | 0.0 | −2.217 | 0.0 | −2.295 | 0.0 |
| | | $L$ | 0.606 | 0.0 | 0.512 | 0.0 | 0.423 | 0.0 | 0.347 | 0.0 |
| | II | $V$ | −1.956 | −0.161 | −2.108 | −0.157 | −2.217 | −0.148 | −2.295 | −0.138 |
| | | $L$ | 0.606 | −0.059 | 0.512 | −0.041 | 0.423 | −0.029 | 0.347 | −0.021 |
| | III | $V$ | −1.955 | −0.161 | −2.109 | −0.157 | −2.219 | −0.148 | −2.296 | −0.138 |
| | | $L$ | 0.597 | −0.059 | 0.507 | −0.041 | 0.419 | −0.029 | 0.344 | −0.021 |

TABLE V. Partial photoionization cross sections (in units of Mb) for the $2p \rightarrow ks$ ($\sigma_s$) and $2p \rightarrow kd$ ($\sigma_d$) transitions in the dipole-velocity calculation.

| | | Ne | | $Na^+$ | | $Mg^{++}$ | | $Al^{+++}$ | |
|---|---|---|---|---|---|---|---|---|---|
| $k$ | Step | $\sigma_s$ | $\sigma_d$ | $\sigma_s$ | $\sigma_d$ | $\sigma_s$ | $\sigma_d$ | $\sigma_s$ | $\sigma_d$ |
| 0.3 | I | 1.54 | 3.77 | 0.630 | 5.18 | 0.333 | 4.84 | 0.202 | 4.00 |
| | II | 1.59 | 4.41 | 0.647 | 5.97 | 0.340 | 5.51 | 0.206 | 4.49 |
| | III | 1.59 | 4.64 | 0.647 | 6.25 | 0.340 | 5.69 | 0.206 | 4.60 |
| 0.5 | I | 1.31 | 4.72 | 0.579 | 5.35 | 0.316 | 4.82 | 0.195 | 3.94 |
| | II | 1.35 | 5.54 | 0.595 | 6.17 | 0.323 | 5.47 | 0.199 | 4.43 |
| | III | 1.36 | 5.84 | 0.595 | 6.45 | 0.323 | 5.66 | 0.199 | 4.53 |
| 0.7 | I | 1.05 | 5.61 | 0.514 | 5.49 | 0.293 | 4.75 | 0.185 | 3.85 |
| | II | 1.09 | 6.62 | 0.528 | 6.34 | 0.299 | 5.41 | 0.188 | 4.33 |
| | III | 1.09 | 6.99 | 0.528 | 6.62 | 0.299 | 5.58 | 0.188 | 4.42 |
| 1.3 | I | 0.471 | 6.30 | 0.310 | 5.22 | 0.208 | 4.23 | 0.144 | 3.38 |
| | II | 0.487 | 7.50 | 0.318 | 6.06 | 0.212 | 4.83 | 0.147 | 3.80 |
| | III | 0.487 | 7.87 | 0.318 | 6.28 | 0.212 | 4.94 | 0.147 | 3.86 |
| 1.9 | I | 0.204 | 4.65 | 0.168 | 3.95 | 0.132 | 3.26 | 0.102 | 2.66 |
| | II | 0.210 | 5.52 | 0.172 | 4.59 | 0.135 | 3.72 | 0.104 | 3.00 |
| | III | 0.209 | 5.65 | 0.172 | 4.67 | 0.135 | 3.77 | 0.104 | 3.02 |
| 2.5 | I | 0.093 | 2.64 | 0.089 | 2.47 | 0.080 | 2.20 | 0.068 | 1.90 |
| | II | 0.095 | 3.09 | 0.091 | 2.85 | 0.081 | 2.50 | 0.069 | 2.13 |
| | III | 0.095 | 3.09 | 0.091 | 2.86 | 0.081 | 2.50 | 0.069 | 2.14 |
| 3.1 | I | 0.046 | 1.29 | 0.049 | 1.37 | 0.048 | 1.34 | 0.044 | 1.25 |
| | II | 0.046 | 1.48 | 0.049 | 1.56 | 0.048 | 1.52 | 0.045 | 1.40 |
| | III | 0.046 | 1.46 | 0.049 | 1.55 | 0.048 | 1.51 | 0.045 | 1.39 |

TABLE VI. Partial photoionization cross sections (in units of Mb) for the $2p \rightarrow ks$ ($\sigma_s$) and $2p \rightarrow kd$ ($\sigma_d$) transitions in the dipole-length calculation.

| | | Ne | | $Na^+$ | | $Mg^{++}$ | | $Al^{+++}$ | |
|---|---|---|---|---|---|---|---|---|---|
| $k$ | Step | $\sigma_s$ | $\sigma_d$ | $\sigma_s$ | $\sigma_d$ | $\sigma_s$ | $\sigma_d$ | $\sigma_s$ | $\sigma_d$ |
| 0.3 | I | 1.65 | 5.12 | 0.677 | 6.81 | 0.358 | 6.23 | 0.218 | 5.06 |
| | II | 1.61 | 4.79 | 0.662 | 6.30 | 0.351 | 5.75 | 0.214 | 4.66 |
| | III | 1.61 | 4.90 | 0.661 | 6.44 | 0.351 | 5.84 | 0.214 | 4.70 |
| 0.5 | I | 1.40 | 6.41 | 0.623 | 7.04 | 0.340 | 6.21 | 0.210 | 4.99 |
| | II | 1.36 | 5.97 | 0.609 | 6.49 | 0.334 | 5.71 | 0.206 | 4.59 |
| | III | 1.36 | 6.10 | 0.608 | 6.63 | 0.334 | 5.80 | 0.206 | 4.63 |
| 0.7 | I | 1.12 | 7.66 | 0.554 | 7.25 | 0.316 | 6.15 | 0.199 | 4.89 |
| | II | 1.09 | 7.06 | 0.541 | 6.66 | 0.310 | 5.64 | 0.196 | 4.49 |
| | III | 1.09 | 7.23 | 0.541 | 6.79 | 0.309 | 5.71 | 0.196 | 4.52 |
| 1.3 | I | 0.517 | 8.95 | 0.340 | 7.09 | 0.226 | 5.57 | 0.156 | 4.33 |
| | II | 0.497 | 7.92 | 0.331 | 6.36 | 0.221 | 5.03 | 0.154 | 3.94 |
| | III | 0.496 | 8.04 | 0.331 | 6.43 | 0.221 | 5.06 | 0.153 | 3.94 |
| 1.9 | I | 0.231 | 6.96 | 0.188 | 5.55 | 0.145 | 4.38 | 0.111 | 3.47 |
| | II | 0.220 | 5.89 | 0.182 | 4.83 | 0.141 | 3.89 | 0.109 | 3.11 |
| | III | 0.220 | 5.84 | 0.182 | 4.80 | 0.141 | 3.86 | 0.109 | 3.09 |
| 2.5 | I | 0.103 | 3.99 | 0.099 | 3.54 | 0.088 | 3.00 | 0.074 | 2.50 |
| | II | 0.098 | 3.25 | 0.096 | 2.99 | 0.085 | 2.60 | 0.073 | 2.21 |
| | III | 0.098 | 3.15 | 0.096 | 2.92 | 0.085 | 2.56 | 0.073 | 2.18 |
| 3.1 | I | 0.048 | 1.91 | 0.053 | 1.95 | 0.052 | 1.84 | 0.048 | 1.66 |
| | II | 0.046 | 1.51 | 0.051 | 1.61 | 0.050 | 1.56 | 0.047 | 1.44 |
| | III | 0.046 | 1.46 | 0.051 | 1.56 | 0.050 | 1.52 | 0.047 | 1.41 |

addition, the effect of the interchannel interaction on the $3p \rightarrow kd$ transition in the Ar sequence also warrants further investigation.

ACKNOWLEDGMENT

I am grateful to Professor U. Fano for many helpful discussions.

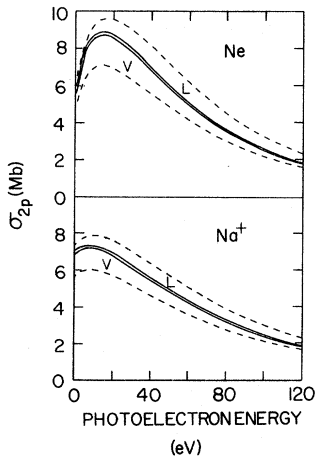


FIG. 5. Partial-photoionization cross section of the $2p$ subshell for Ne and $Na^+$. The solid lines and the dashed lines represent the results of step III and step I, respectively.

## APPENDIX A

Most of the numerical techniques used in the present calculation are straightforward. In the following, we briefly outline one of the numerical procedures which we have developed to solve the inhomogeneous differential equation (2b) in Ref. 7. The inhomogeneous equation takes the general form

$$[h(r) - \epsilon]\phi(r) = g(r), \tag{A1}$$

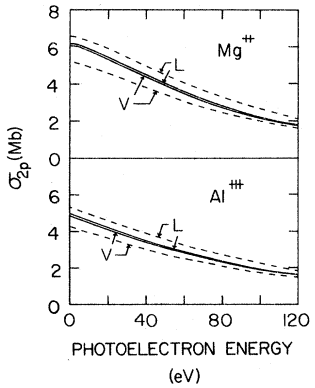


FIG. 6. Partial-photoionization cross section of the $2p$ subshell for $Mg^{++}$ and $Al^{+++}$. The solid lines and the dashed lines represent the results of step III and step I, respectively.

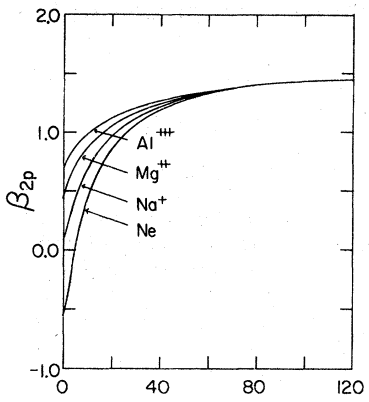


FIG. 7. Asymmetry parameter $\beta_{2p}$ for Ne isoelectronic sequence. Only the length results in step III of the present calculation are given.

where $h(r)$ is the effective Hamiltonian, $g(r)$ is the inhomogeneous part, and $\epsilon$ is a negative constant. The boundary conditions for $\phi(r)$ are (i) $\phi(r) \to r^{l+1}$ as $r \to 0$ and (ii) $\phi(r) \to 0$ as $r \to \infty$.

Similar to a numerical procedure which we developed earlier[16] to solve the same equation with positive $\epsilon$, we write the solution of Eq. (A1),

$$\phi(r) = A\phi^h(r) + \phi^p(r). \tag{A2}$$

To obtain $\phi$, we first solve

$$[h(r) - \epsilon]\phi^h(r) = 0, \tag{A3}$$

with an arbitrary choice of initial expansion coefficient. Secondly, we obtain function $\phi^p(r)$ by solving Eq. (A1), again, with an arbitrary choice of initial expansion coefficient. From the second boundary condition, we find numerically that

$$A = -\phi^p(r=R)/\phi^h(r=R), \tag{A4}$$

where $R$, the maximum $r$ of integration, is chosen to be large enough such that

$$\phi(r=R) \cong 0. \tag{A5}$$

$R$ is usually determined by the absolute value of $\epsilon$ and the range of the inhomogeneous part. Thus, we obtain the solution $\phi(r)$ from Eq. (A2) with the calculated $\phi^p(r)$, $\phi^h(r)$, and $A$. The nonlocal part in the Hamiltonian is included by the usual iterative procedure. We note here that despite the fact that both $\phi^p$ and $\phi^h$ are divergent at large $r$, the solution $\phi$ satisfies both boundary conditions.

[1]C. F. Barnett, *The Physics of Electronic and Atomic Collisions (IX ICPEAC)*, edited by J. S. Risley and R. Geballe (Univ. of Washington, Seattle, 1976), p. 846.
[2]For example, see "Beam Foil Spectroscopy" (Proceedings of the Third International Conference on Beam-Foil Spectroscopy, Tucson), edited by S. Bashkin, Nucl. Instrum. Methods 110, 1 (1973).
[3]T. B. Lucatorto and T. J. McIlrath, Phys. Rev. Lett. 37, 428 (1976).
[4]D. J. Pegg, S. B. Elston, P. M. Griffin, H. C. Hayden, J. P. Forester, R. S. Thoe, R. S. Peterson, and I. A. Sellin, Phys. Rev. A 14, 1036 (1976).
[5]T. N. Chang and U. Fano, Phys. Rev. A 13, 263 (1976).
[6]T. N. Chang and U. Fano, Phys. Rev. A 13, 282 (1976).
[7]T. N. Chang, Phys. Rev. A 15, 2392 (1977).
[8]J. Cooper and R. N. Zare, *Lectures in Theoretical Physics 11c*, edited by S. Geltman, K. Mahanthappa, and N. Brittin (Gordon and Preach, New York, 1969), p. 317.
[9]D. J. Kennedy and S. T. Manson, Phys. Rev. A 5, 227 (1972).
[10]Only those dominant many-body effects discussed in Refs. 5 and 7 are included in the present calculation.
[11]Y. Hahn and K. M. Watson, Phys. Rev. A 7, 491 (1973); Y. Hahn, *ibid.* 13, 1326 (1976).
[12]U. Fano and M. Inokuti, Argonne Nat. Lab. Report No. ANL-76-80 (1976) (unpublished).
[13]F. Combet Farnoux and M. Lamoureux, J. Phys. B 9, 897 (1976).
[14]A. Msezane, R. F. Reilman, S. T. Manson, J. R. Swanson, and L. Armstrong, Phys. Rev. A 15, 668 (1977).
[15]J. R. Swanson and L. Armstrong, Phys. Rev. A 15, 661 (1977).
[16]T. N. Chang and R. T. Poe, J. Comp. Phys. 12, 557 (1973).